JOURNAL OF GUIDANCE, CONTROL, AND DYNAMICS
Vol. 33, No. 1, January–February 2010

Engineering Notes

Backstepping Control Design with Actuator Torque Bound for Spacecraft Attitude Maneuver

Imran Ali,* Gianmarco Radice,† and Jongrae Kim‡
University of Glasgow,
Glasgow, Scotland G12 8QQ, United Kingdom

DOI: 10.2514/1.45541

Introduction

BACKSTEPPING is a popular nonlinear control design technique [1,2]. It hinges on using a part of the system states as virtual controls to control the other states. Generating a family of globally asymptotically stabilizing control laws is the main advantage of this method that can be exploited for addressing robustness issues and solving adaptive problems. The term backstepping refers to the recursive nature of the control design procedure in which a control law and a control Lyapunov function are recursively constructed to guarantee stability. Backstepping has been considered for the spacecraft slew maneuvers [3,4]. The cascaded structure of spacecraft kinematics and dynamics makes the integrator backstepping a preferred approach for the spacecraft attitude maneuver problem, resulting in smooth feedback controls [5]. However, the typical control actuators used for this problem (such as reaction wheels, control moment gyros, or thrusters) have an upper bound on the control torque they can exert onto the system and the simple or conventional backstepping control method may result in excessive control input beyond that saturation bound. The issue has been addressed in the literature using other control methodologies such as nonlinear proportional–integral–derivative control [6], Lyapunov-optimal control [7] and variable structure control [8–11].

In this work, we design a nonlinear backstepping attitude controller using the inverse tangent-based tracking function [4] and a family of augmented Lyapunov functions [12]. Using this control law, we derive an analytical upper bound of the control torque norm. The bound is effectively used to tune the control parameters so that, for the given settling time specification, the upper bound of the control input is minimized. The performance of the proposed controller has shown improvements in minimizing the peak control torque and the settling time.

The rest of the Note is organized as follows: First, the kinematics and dynamics of rigid spacecraft are summarized. Second, the details of the design procedure for the proposed controller and the analytical bounds for the control torque components are given. Third, the efficacy of the proposed scheme is demonstrated by the numerical simulations for the cases of attitude stabilization and tracking both. Finally, the conclusions are presented.

Received 19 May 2009; revision received 27 July 2009; accepted for publication 31 August 2009.

*Ph.D. Student, James Watt (South) Building, Department of Aerospace Engineering; iali@aero.gla.ac.uk.

†Senior Lecturer, James Watt (South) Building, Department of Aerospace Engineering; gradice@aero.gla.ac.uk.

‡Lecturer, James Watt (South) Building, Department of Aerospace Engineering; jkim@aero.gla.ac.uk.

Rigid Spacecraft Attitude Motion

First, we introduce various frames that will be used in the following developments. The spacecraft is assumed to be a rigid body and three mutually perpendicular axes fixed in the spacecraft define a body frame **B** with origin at the center of mass of the spacecraft. The spacecraft is assumed to be equipped with the actuators that can provide torques about the axes of the body frame **B**. Let **N** be an inertial frame. The orientation of the body frame **B** with respect to the inertial frame **N** is represented by the quaternion $\boldsymbol{q} = [\,\boldsymbol{q}_v^T, \quad q_4\,]^T$, where $\boldsymbol{q}_v \in \Re^3, q_4 \in \Re$, and $\boldsymbol{q}_v^T\boldsymbol{q}_v + q_4^2 = 1$. Here, $\Re$ is the real number set. The reference frame corresponding to the commanded motion is denoted by $\tilde{\mathbf{R}}$ and its attitude with respect to the inertial frame **N** is specified by the quaternion $\boldsymbol{q}_r = [\,\boldsymbol{q}_{rv}^T, \quad q_{r4}\,]^T$. The quaternion $\tilde{\boldsymbol{\sigma}} = [\,\tilde{\boldsymbol{\sigma}}_v^T, \quad \tilde{\sigma}_4\,]^T$ describes the orientation of the body frame **B** with respect to the reference frame $\tilde{\mathbf{R}}$ and is written as

$$\tilde{\boldsymbol{\sigma}}_v = q_{r4}\boldsymbol{q}_v - q_4\boldsymbol{q}_{rv} - \boldsymbol{q}_{rv} \times \boldsymbol{q}_v \qquad \tilde{\sigma}_4 = \boldsymbol{q}_{rv}^T\boldsymbol{q}_v + q_{r4}q_4 \tag{1}$$

Let **P** represent the spacecraft principal-axis frame. We choose to define a pseudoreference frame **R**, which is rigidly connected to the reference frame $\tilde{\mathbf{R}}$ and is misaligned with it in the same way as the principal-axis frame **P** with the body frame **B**. The attitude tracking error is taken as $\boldsymbol{\sigma} = [\,\boldsymbol{\sigma}_v^T, \quad \sigma_4\,]^T$, which is the quaternion representing the attitude of the principal-axis frame **P** relative to the pseudoreference frame **R**. If **S** denotes the direction cosine matrix of the principal-axis frame **P** relative to the body frame **B**, then $\boldsymbol{\sigma}_v = \mathbf{S}\tilde{\boldsymbol{\sigma}}_v$ and $\sigma_4 = \tilde{\sigma}_4$. With the mentioned choice for the definition of attitude tracking error, the coincidence of the principal-axis frame **P** with the pseudoreference frame **R** makes the body frame **B** align to the reference frame $\tilde{\mathbf{R}}$. A graphical description of all the aforesaid frames is available as Fig. 1. The equations of rotational motion of the spacecraft are given by [13]

$$\dot{\boldsymbol{q}}_v = \tfrac{1}{2}(q_4\tilde{\boldsymbol{\omega}} - \tilde{\boldsymbol{\omega}} \times \boldsymbol{q}_v), \qquad \dot{q}_4 = -\tfrac{1}{2}\tilde{\boldsymbol{\omega}}^T\boldsymbol{q}_v \tag{2}$$

$$\mathbf{J}_B\dot{\tilde{\boldsymbol{\omega}}} + \tilde{\boldsymbol{\omega}} \times [\mathbf{J}_B\tilde{\boldsymbol{\omega}}] = \boldsymbol{T}_B \tag{3}$$

where $\tilde{\boldsymbol{\omega}} = [\tilde{\omega}_1, \tilde{\omega}_2, \tilde{\omega}_3]^T$ is the angular velocity of the spacecraft with respect to the inertial frame **N** expressed in the body frame **B**, $\mathbf{J}_B = \mathbf{J}_B^T$ is the body frame **B** referenced positive definite inertia matrix of the spacecraft, $\boldsymbol{T}_B$ is the control torque vector in the body frame **B**, and the superscript T is the transpose of the vector or matrix. We define the three subscripts (i, j, and k) as the element of the set Id as follows: $(i, j, k) \in \mathrm{Id}$, where $\mathrm{Id} = \{(1,2,3), \quad (2,3,1), \quad (3,1,2)\}$. The first part of Eq. (2) can be written as

$$\dot{q}_i = \frac{1}{2}(q_4\tilde{\omega}_i - q_k\tilde{\omega}_j + q_j\tilde{\omega}_k) \tag{4}$$

for $(i, j, k) \in \mathrm{Id}$.

Let us have $\boldsymbol{\omega} = \mathbf{S}\tilde{\boldsymbol{\omega}}$, $\boldsymbol{T} = \mathbf{S}\boldsymbol{T}_B$, and $\mathbf{J} = \mathbf{S}\mathbf{J}_B\mathbf{S}^T$, where $\boldsymbol{\omega} = [\omega_1, \omega_2, \omega_3]^T$, $\boldsymbol{T} = [T_1, T_2, T_3]^T$, and $\mathbf{J} = \mathrm{diag}(J_1, J_2, J_3)$. For the principal-axis frame **P**, Eq. (3) becomes

$$\dot{\omega}_i = p_i\omega_j\omega_k + u_i \tag{5}$$

where $p_i = (J_j - J_k)/J_i$ and $u_i = T_i/J_i$, for $(i, j, k) \in \mathrm{Id}$. Further, the spacecraft principal-axis frame **P** is desired to track the attitude motion of the pseudoreference frame **R**, for which the angular

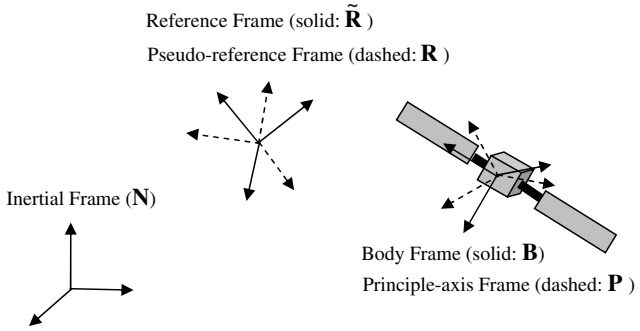

Fig. 1 Relations between the used frames: The pseudoreference frame R is rigidly connected to the reference frame $\tilde{\mathbf{R}}$ and is misaligned with it in the same way as the principle-axis frame P with the body frame B.

velocity and angular acceleration relative to the inertial frame **N** expressed in the principal-axis frame **P** are denoted by $\boldsymbol{\omega}_r = [\omega_1^r, \omega_2^r, \omega_3^r]^T$ and $\dot{\boldsymbol{\omega}}_r = [\dot{\omega}_1^r, \dot{\omega}_2^r, \dot{\omega}_3^r]^T$, respectively. The angular velocity tracking error is written as

$$\delta\boldsymbol{\omega} = \boldsymbol{\omega} - \boldsymbol{\omega}_r \tag{6}$$

whereas for the angular acceleration tracking error, we have

$$\frac{{}^P d}{dt}(\delta\boldsymbol{\omega}) = \dot{\boldsymbol{\omega}} - \dot{\boldsymbol{\omega}}_r + \boldsymbol{\omega} \times \boldsymbol{\omega}_r \tag{7}$$

where

$$\frac{{}^P d}{dt}(\delta\boldsymbol{\omega}) = [\delta\dot{\omega}_1, \delta\dot{\omega}_2, \delta\dot{\omega}_3]^T$$

represents the derivative of $\delta\boldsymbol{\omega}$ as seen by the principal-axis frame **P** [14]. Equations (5) and (7) can be used to write the tracking error dynamics equation as

$$\delta\dot{\omega}_i = p_i\omega_j\omega_k + u_i - \dot{\omega}_i^r + \omega_j\omega_k^r - \omega_k\omega_j^r \tag{8}$$

for $(i, j, k) \in \mathrm{Id}$. Finally, the attitude tracking control objective becomes the regulation of $\lim_{t\to\infty}[\boldsymbol{\sigma}_v(t), \delta\boldsymbol{\omega}(t)] = \mathbf{0}$.

Control Design and Torque Bound

The candidate Lyapunov function for the kinematics subsystem stabilization is

$$V = \frac{1}{2}[\sigma_1^2 + \sigma_2^2 + \sigma_3^2 + (1 - \sigma_4)^2] \tag{9}$$

which is continuously differentiable and zero at the equilibrium point $\boldsymbol{\sigma}_v = \mathbf{0}$ and $\sigma_4 = 1$. The time derivative of V comes out to be

$$\dot{V} = \frac{1}{2}\sum_{i=1}^{3}\sigma_i\delta\omega_i \tag{10}$$

For stabilizing the kinematics subsystem, the pseudocontrol input $\delta\omega_i^s$ is based on a nonlinear tracking function $\phi(\sigma_i)$, as follows [4]:

$$\delta\omega_i^s = -s\phi(\sigma_i) \tag{11}$$

where s is a positive constant and the nonlinear tracking function $\phi(\sigma_i)$ is given by

$$\phi(\sigma_i) = \alpha\tan^{-1}(\beta\sigma_i) \tag{12}$$

with α and β as positive constants. This choice of the pseudocontrol for the kinematics subsystem achieves the objective of $\lim_{t\to\infty}\boldsymbol{\sigma}_v(t) = \mathbf{0}$ as it makes the time derivative of the Lyapunov function V given by Eq. (10) as the negative semidefinite as follows:

$$\dot{V} = -\frac{1}{2}s\sum_{i=1}^{3}\sigma_i\phi(\sigma_i) \tag{13}$$

Further, it can be shown that the convergence to $\boldsymbol{\sigma}_v = \mathbf{0}$ and $\sigma_4 = 1$ is achieved asymptotically for all initial conditions $\boldsymbol{\sigma}(t_0)$ whenever the initial condition $\sigma_4(t_0) \neq -1$, where t_0 is the initial time [15]. Next,

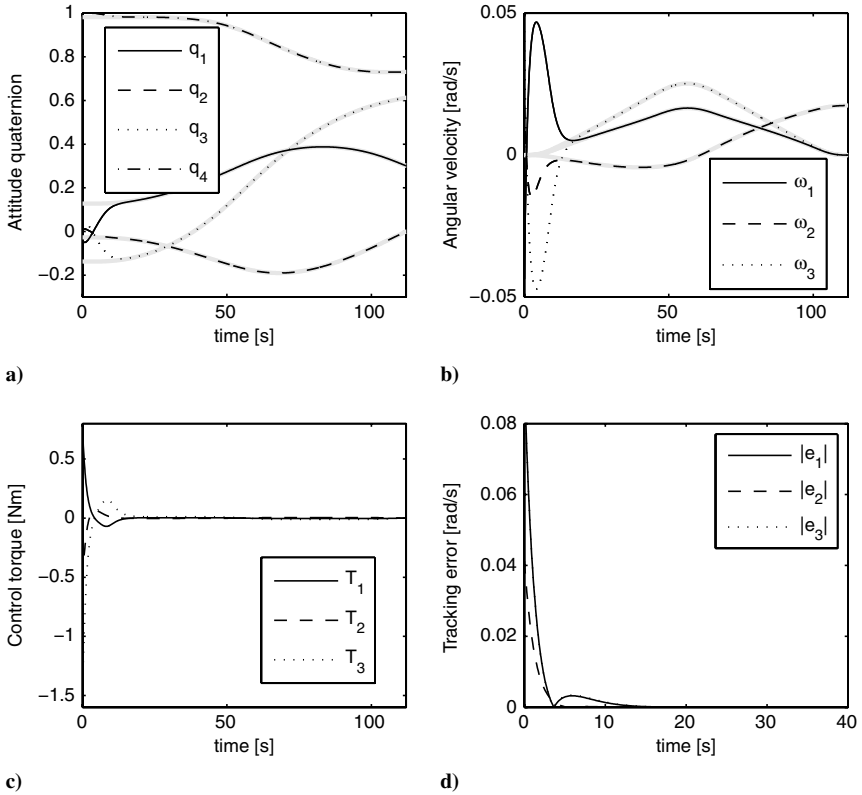

Fig. 2 Simulation results for the tracking case example: a) quaternion, b) angular velocity, c) control torque, and d) angular velocity tracking error histories. (Gray lines represent the reference command.)

the function V is augmented with the dynamics part of the system as follows [12]:

$$U = V + \frac{1}{2}\sum_{i=1}^{3}[\Omega(\delta\omega_i) - \Omega(\delta\omega_i^s)]^2 \tag{14}$$

where $\Omega(\cdot)$ is a class κ_∞ function (i.e., it is zero at zero, strictly increasing and becomes unbounded as its argument increases to infinity) [12]. The time derivative of the overall Lyapunov function U yields

$$\begin{aligned}\dot{U} &= \frac{1}{2}\sum_{i=1}^{3}\sigma_i\delta\omega_i + \sum_{i=1}^{3}[\Omega(\delta\omega_i) - \Omega(\delta\omega_i^s)][\Omega'(\delta\omega_i)\delta\dot{\omega}_i \\ &\quad - \Omega'(\delta\omega_i^s)\delta\dot{\omega}_i^s] = \frac{1}{2}\sum_{i=1}^{3}\sigma_i\delta\omega_i^s + \sum_{i=1}^{3}\frac{1}{2}\sigma_i(\delta\omega_i - \delta\omega_i^s) \\ &\quad + \sum_{i=1}^{3}[\Omega'(\delta\omega_i)(p_i\omega_j\omega_k + u_i - \dot{\omega}_i^r + \omega_j\omega_k^r - \omega_k\omega_j^r) \\ &\quad - \Omega'(\delta\omega_i^s)\delta\dot{\omega}_i^s][\Omega(\delta\omega_i) - \Omega(\delta\omega_i^s)] = -\frac{1}{2}s\sum_{i=1}^{3}\sigma_i\phi(\sigma_i) \\ &\quad + \sum_{i=1}^{3}\left\{\frac{1}{2}\sigma_i + [\Omega'(\delta\omega_i)(p_i\omega_j\omega_k + u_i - \dot{\omega}_i^r + \omega_j\omega_k^r - \omega_k\omega_j^r)\right. \\ &\quad \left. - \Omega'(\delta\omega_i^s)\delta\dot{\omega}_i^s]\frac{\Omega(\delta\omega_i) - \Omega(\delta\omega_i^s)}{\delta\omega_i - \delta\omega_i^s}\right\}(\delta\omega_i - \delta\omega_i^s)\end{aligned} \tag{15}$$

where $\Omega(x)$ is chosen such that

$$[\Omega(\delta\omega_i) - \Omega(\delta\omega_i^s)]/(\delta\omega_i - \delta\omega_i^s) \neq 0$$

and $\Omega'(x)$ denotes the derivative of $\Omega(x)$ with respect to x. In order to make the time derivative of U equal to the following

$$\dot{U} = -\frac{1}{2}s\sum_{i=1}^{3}\sigma_i\phi(\sigma_i) - g\sum_{i=1}^{3}(\delta\omega_i - \delta\omega_i^s)^2 \tag{16}$$

the backstepping controller comes out to be

$$\begin{aligned}u_i &= \frac{1}{\Omega'(\delta\omega_i)}\left\{-\frac{\delta\omega_i - \delta\omega_i^s}{\Omega(\delta\omega_i) - \Omega(\delta\omega_i^s)}\left[\frac{1}{2}\sigma_i + g(\delta\omega_i - \delta\omega_i^s)\right]\right. \\ &\quad \left. + \Omega'(\delta\omega_i^s)\delta\dot{\omega}_i^s\right\} - p_i\omega_j\omega_k + \dot{\omega}_i^r - \omega_j\omega_k^r + \omega_k\omega_j^r\end{aligned} \tag{17}$$

for $(i, j, k) \in \mathrm{Id}$, where g is a positive constant.

For the closed-loop system, the attitude tracking control objective $\lim_{t\to\infty}[\boldsymbol{\sigma}_v(t), \delta\boldsymbol{\omega}(t)] = \mathbf{0}$ is achieved almost globally and asymptotically, as Eq. (16) is negative semidefinite. The standard terminology of almost global stability for this problem means stability over an open and dense set in the set of the special group of rotation matrices that describe spacecraft orientation in three dimensions $SO(3)$ [16,17]. This is because of the well-known fact that $SO(3)$ is not a contractible space, and hence the quaternion-based controllers do not offer globally continuous stabilizing formulations [18,19].

Note that by equating Eqs. (15) and (16) we can find the time derivative of $U - V$ as given below, which is subject to the condition that the control input is given by Eq. (17):

$$\frac{d}{dt}\left(\frac{1}{2}[\Omega(\delta\omega_i) - \Omega(\delta\omega_i^s)]^2\right) = -g(\delta\omega_i - \delta\omega_i^s)^2 - \frac{1}{2}\sigma_i(\delta\omega_i - \delta\omega_i^s) \tag{18}$$

for $i = 1, 2, 3$.

We choose a simple form of class κ_∞ function as $\Omega(\delta\omega_i) = \eta\delta\omega_i$ with $\eta > 0$, which satisfies the condition

$$[\Omega(\delta\omega_i) - \Omega(\delta\omega_i^s)]/(\delta\omega_i - \delta\omega_i^s) = \eta \neq 0$$

for $i = 1, 2, 3$. Then the control input is rewritten as follows:

$$\begin{aligned}u_i &= -\frac{1}{\eta^2}\left[\frac{1}{2}\sigma_i + g(\delta\omega_i - \delta\omega_i^s)\right] - \frac{1}{2}s\phi'(\sigma_i)(\sigma_4\delta\omega_i - \sigma_k\delta\omega_j \\ &\quad + \sigma_j\delta\omega_k) - p_i\omega_j\omega_k + \dot{\omega}_i^r - \omega_j\omega_k^r + \omega_k\omega_j^r\end{aligned} \tag{19}$$

for $(i, j, k) \in \mathrm{Id}$, where $\phi'(\sigma_i)$ is the derivative of $\phi(\sigma_i)$ with respect to σ_i. Defining $e_i \equiv \delta\omega_i - \delta\omega_i^s$, the above equation can be written as

$$\begin{aligned}u_i &= -\frac{1}{\eta^2}\left[\frac{1}{2}\sigma_i + ge_i\right] - \frac{1}{2}s\phi'(\sigma_i)(\sigma_4 e_i - \sigma_k e_j + \sigma_j e_k + \sigma_4\delta\omega_i^s \\ &\quad - \sigma_k\delta\omega_j^s + \sigma_j\delta\omega_k^s) - p_i(e_j + \delta\omega_j^s + \omega_j^r)(e_k + \delta\omega_k^s + \omega_k^r) \\ &\quad + \dot{\omega}_i^r - (e_j + \delta\omega_j^s)\omega_k^r + (e_k + \delta\omega_k^s)\omega_j^r\end{aligned} \tag{20}$$

As $|\sigma_i| \le 1$, $|\delta\omega_i^s| \le s\alpha\tan^{-1}(\beta)$, $|\phi'(\sigma_i)| \le \alpha\beta$, $|\omega_i^r| \le \xi$, and $|\dot{\omega}_i^r| \le \gamma$ for $i = 1, 2, 3$, the control torque bound is derived using the triangle inequalities as follows:

$$\begin{aligned}|u_i| &\le \frac{1}{\eta^2}\left(\frac{1}{2}|\sigma_i| + g|e_i|\right) + \frac{1}{2}s|\phi'(\sigma_i)||\sigma_4 e_i - \sigma_k e_j + \sigma_j e_k \\ &\quad + \sigma_4\delta\omega_i^s - \sigma_k\delta\omega_j^s + \sigma_j\delta\omega_k^s| + |p_i(e_j + \delta\omega_j^s + \omega_j^r)(e_k + \delta\omega_k^s \\ &\quad + \omega_k^r)| + |\dot{\omega}_i^r| + |(e_j + \delta\omega_j^s)\omega_k^r| + |(e_k + \delta\omega_k^s)\omega_j^r| \\ &\le \frac{1}{\eta^2}\left(\frac{1}{2} + g|e_i|\right) + \frac{1}{2}s\alpha\beta(|\sigma_4 e_i| + |\sigma_k e_j| + |\sigma_j e_k| \\ &\quad + |\sigma_4\delta\omega_i^s| + |\sigma_k\delta\omega_j^s| + |\sigma_j\delta\omega_k^s|) + |p_i||e_j e_k + e_j\delta\omega_k^s + e_j\omega_k^r \\ &\quad + \delta\omega_j^s e_k + \delta\omega_j^s\delta\omega_k^s + \delta\omega_j^s\omega_k^r + \omega_j^r e_k + \omega_j^r\delta\omega_k^s + \omega_j^r\omega_k^r| \\ &\quad + |\dot{\omega}_i^r| + |e_j + \delta\omega_j^s||\omega_k^r| + |e_k + \delta\omega_k^s||\omega_j^r| \\ &\le \frac{1}{\eta^2}\left(\frac{1}{2} + g|e_i|\right) + \frac{1}{2}s\alpha\beta(|e_i| + |e_j| + |e_k| + 3s\alpha\tan^{-1}(\beta)) \\ &\quad + |p_i|\{|e_j||e_k| + (\xi + s\alpha\tan^{-1}(\beta))(|e_j| + |e_k| \\ &\quad + s\alpha\tan^{-1}(\beta)) + \xi s\alpha\tan^{-1}(\beta) + \xi^2\} + \gamma + (|e_j| + |e_k| \\ &\quad + 2s\alpha\tan^{-1}(\beta))\xi\end{aligned}$$

for $(i, j, k) \in \mathrm{Id}$. Rearranging the terms, the inequality becomes

$$|u_i| \le k_{1i} + k_2|e_i| + k_{3i}(|e_j| + |e_k|) + |p_i||e_j||e_k| \tag{21}$$

for $(i, j, k) \in \mathrm{Id}$, where the constants k_{1i}, k_2, and k_{3i} are

$$k_{1i} = \frac{1}{2\eta^2} + \left(\frac{3}{2}s\alpha\beta + 2\xi\right)s\alpha\tan^{-1}(\beta) + |p_i|(\xi + s\alpha\tan^{-1}(\beta))^2 + \gamma$$

$$k_2 = \frac{g}{\eta^2} + \frac{1}{2}s\alpha\beta \qquad k_{3i} = s\alpha\left(\frac{1}{2}\beta + |p_i|\tan^{-1}(\beta)\right) + (|p_i| + 1)\xi$$

However, the angular rate error $e_i(t)$, for $i = 1, 2, 3$, is unknown in Eq. (21). Hence, Eq. (21) does not give any useful information about the control torque bound. To obtain the bound for the angular rate error, recall Eq. (18) with $\Omega(\delta\omega_i) = \eta\delta\omega_i$ for $i = 1, 2, 3$. Then,

$$\eta^2\frac{d}{dt}\left(\frac{1}{2}e_i^2\right) = -ge_i^2 - \frac{1}{2}\sigma_i e_i \tag{22}$$

for $i = 1, 2, 3$. Equation (22) implies that if $|e_i| > |\sigma_i|/(2g)$, then $|e_i|$ is guaranteed to be decreasing to a certain value that is bounded by $1/(2g)$. Therefore, $|e_i|$ is bounded by the following inequality:

$$|e_i(t)| \le \max[|e_i(t_0)|, 1/(2g)] \tag{23}$$

for all t in $[t_0, \infty)$ for $i = 1, 2, 3$, where t_0 is the initial time and $\max(,)$ is the function for which the value is the maximum of two arguments.

Finally, Eq. (21) is used to calculate the bounds of the controls u_i and the control torque is bounded by

$$\begin{aligned}|T_i| &\le J_i[k_{1i} + k_2|e_i(t)| + k_{3i}(|e_j(t)| + |e_k(t)|) \\ &\quad + |p_i||e_j(t)||e_k(t)|]\end{aligned} \tag{24}$$

for $(i, j, k) \in \mathrm{Id}$, where $|e_i(t)|$ for $i = 1, 2, 3$ follows the inequality (23). Hence, the minimum value of the bound for $|T_i|$ identifiable by Eq. (24) comes out to be

$$J_i\left[k_{1i} + \frac{1}{2g}\left(k_2 + 2k_{3i} + \frac{1}{2g}|p_i|\right)\right]$$

The control torque components bounds given by Eq. (24) can be used to calculate the bound for Euclidean norm $\|\boldsymbol{T}\|_2$. Moreover, the direction cosine matrix $\mathbf{S}$ mentioned in the previous section can be used to calculate $\boldsymbol{T}_B$ from $\boldsymbol{T}$; however, this transformation does not affect the bound for the Euclidean-norm of control torque.

Numerical Simulation

Stabilization Case

If the reference frame $\tilde{\mathbf{R}}$ coincides with the inertial frame $\mathbf{N}$ (i.e., $\boldsymbol{\omega}_r(t) = \mathbf{0}, \boldsymbol{q}_r(t) = [0 \quad 0 \quad 0 \quad 1]^T, \xi = 0$, and $\gamma = 0$) then the problem is reduced to attitude stabilization. The effectiveness of the proposed backstepping controller for the case of attitude stabilization is evaluated through the numerical simulation of a rest-to-rest slew maneuver. The same simulation scenario as considered in [3,4] is used as follows:

$$\mathbf{J} = \mathrm{diag}(10, 15, 20)\ \mathrm{kg \cdot m^2}$$

$$\boldsymbol{q}(t_0) = [0.4646 \quad 0.1928 \quad 0.8047 \quad 0.3153]^T$$

$$\boldsymbol{q}(t_f) = [0 \quad 0 \quad 0 \quad 1]^T$$

where t_0 and t_f are the starting and the final times, respectively. For the sake of comparison, all of the following values are adopted from [4]: $s = 1$, $g = 10$, $\alpha = 0.75$, and $\beta = 8.0$. For the given values, the control torque bounds are obtained using Eq. (24) as follows:

$$|T_1| \le \frac{103}{\eta^2} + 201 \qquad |T_2| \le \frac{120}{\eta^2} + 316$$

$$|T_3| \le \frac{222}{\eta^2} + 382\ \mathrm{N \cdot m} \tag{25}$$

Hence, the Euclidean-norm bound is given by

$$\|\boldsymbol{T}\|_2 \le 535\sqrt{\frac{1.0}{\eta^4} + \frac{0.26}{\eta^2} + 1}\ \mathrm{N \cdot m} \tag{26}$$

For comparison with the results of [4], the gain η is tuned so that for the considered rest-to-test maneuver, the value for $\max(\|\boldsymbol{T}\|_2)$ becomes 21.6 N · m, where $\max(\|\boldsymbol{T}\|_2)$ denotes the peak Euclidean norm of the actual control torque from the simulation. By trial and error, η is found to be equal to 3.5196. For the chosen η, the bound given by Eq. (26) becomes about 556 N · m, whereas the settling time t_{settling} comes out to be nearly 5.18 s. Here, t_{settling} is defined as the time such that the norm of the states vector $[\boldsymbol{q}_v^T, \quad \boldsymbol{\omega}^T]^T$ is bounded by 1% error from the steady state, which is zero in this case, for all $t \ge t_{\mathrm{settling}}$. Better performance in the settling time is mainly because of the incorporation of the nonlinear tracking function $\phi(q_i)$, whereas the reduction of the peak control torque has been achieved through the introduction of the constant control gain η. The proposed controller offers adequate performance despite the fact that it has a much simpler form than the one in [4], which uses additional switching parameters to obtain the robustness with respect to the inertia uncertainty. Moreover, as summarized in Table 1, it shows better performance when compared with the other existing methods in [3,20,21].

The bound given by Eq. (26) is very conservative, in that it is about 25 times bigger than the actual maximum torque. This is caused by the short desired settling time as the corresponding control parameters become large to achieve that specification. Moreover, in this case, only one parameter, η, has been tuned. If all five parameters in the bound (i.e., s, g, α, β, and η) are simultaneously used for lowering the bound, the bound will be less conservative. To demonstrate this, the following optimization problem is solved using the sequential quadratic programming (SQP):

$$\min_{\alpha>0.1,\beta>0.1,s>0.1,g>0.1,\eta>0.1} \|\boldsymbol{T}_{\mathrm{analytical}}\|$$

subject to $t_{\mathrm{settling}} \le 5$ s, $\max(\|T\|_2) \le 21.6$ N · m, and the closed-loop differential equations, where $\boldsymbol{T}_{\mathrm{analytical}}$ is the analytical upper bound given by Eq. (24). The lower bounds of s, g, α, β, and η are all set to 0.1, as the values of these parameters smaller than this would hardly achieve the given settling time specification of the closed-loop response. Starting from the aforementioned values of s, g, α, β, and η, the above optimization problem is solved using the SQP. The values of the parameters s, g, α, β, and η converged to 0.34, 1.16, 0.98, 10.9, and 1.01, respectively. The resulting $\|\boldsymbol{T}_{\mathrm{analytical}}\|$ is about 174 N · m, whereas the corresponding $\max(\|\boldsymbol{T}\|_2)$ is 21.6 N · m. The conservativeness of the upper bound is significantly reduced (i.e., from 25 times to just over eight times bigger than the actual maximum torque). Moreover, the optimized bound guarantees that the actual control torque never exceeds the bound, with the condition that $|e_i(t_0)|$ is less than or equal to the value for the current scenario.

It is noteworthy to compare the obtained value of the analytical torque bound even with the simulation values of the peak control torque mentioned in Table 1, where it is almost twice that for [20] and is less than those by [3,4,21]. Here, the linear version of the backstepping controller by [4] is being compared. Moreover, in this study we have exploited the integrator backstepping design methodology for developing analytical bound for the control torque, with the control law given by Eq. (19) being similar in shape to that already existing in the literature [17]. The methodology can be turned to further advantage by exploiting it to avoid the cancellation of good nonlinearities, if any, in the system. It may be helpful to decrease both the peak control torque from the simulation and its analytical bound. As we used a simple local optimization algorithm, the bound may also be improved further with some global optimization techniques.

In the above numerical example, the body axes and the principal axes of the spacecraft are taken as coincident. Otherwise, one can always find the inertia matrix about the principal axes and proceed as mentioned above. Later, the results can be transformed back to the body axes employing the transformation matrix $\mathbf{S}$; however, it does not change the findings regarding the bound for the Euclidean norm of the control torque.

Table 1 Simulation results[a]

Controller	Peak control torque $\max(\|\boldsymbol{T}\|_2)$, N · m	Angular velocity norm $\|\boldsymbol{\omega}\|_2$ at 5 s, rad/s	Quaternion norm $\|\boldsymbol{q}_v\|_2$ at 5 s
Linear backstepping controller [4]	178.4	0.1151	0.1093
Controller in [20]	85.0	0.1170	0.1039
Controller in [21]	311.8	0.1402	0.1957
Controller in [3]	196.2	0.1327	0.2304
Controller in [4]	21.6	5.75e − 4	9.64e − 5
Proposed controller	21.6	10.2e − 3	5.6e − 3

[a]All values are taken from [4], except those for the proposed controller.

Tracking Case

In this subsection, we carry out the numerical simulation of the tracking attitude maneuver in order to demonstrate the proposed control law. The diagonal inertia matrix of the spacecraft has the same entries as considered for the stabilization example. The open-loop reference maneuver is a smoothed near-minimum-time maneuver starting at rest but having a certain angular velocity at the end of the maneuver, as desirable for landmark tracking [7,22]. It takes the spacecraft from the 3-1-3 Euler angles (−20, 15, and 4 deg) or the unit attitude quaternion

$$\boldsymbol{q}_r(t_0) = [\,0.1277 \quad -0.0271 \quad -0.1380 \quad 0.9818\,]^T$$

to the angles (40, 35, and 40 deg) or

$$\boldsymbol{q}_r(t_f) = [\,0.3007 \quad 0 \quad 0.6130 \quad 0.7306\,]^T$$

with a final body angular velocity $\boldsymbol{\omega}_r(t_f) = [\,0 \quad 1 \quad 0\,]^T$ deg/s. For the chosen maneuver, the upper bounds for the absolute values of the reference angular velocity and angular acceleration components are $\xi = 1.7316$ deg/s and $\gamma = 0.0469$ deg/s^2, respectively, and the final maneuver time is $t_f = 112$ s. The initial attitude error in 3-1-3 Euler angles is taken as (10, −20, and 10 deg), resulting in the spacecraft initial attitude quaternion:

$$\boldsymbol{q}(t_0) = [\,-0.0427 \quad 0.0091 \quad 0.0349 \quad 0.9984\,]^T$$

and the initial angular velocity error is chosen to be (−2.5, 1.0 and 2.5 deg/s) leading to the initial spacecraft angular velocity:

$$\boldsymbol{\omega}(t_0) = [\,-2.5 \quad 1.0 \quad 2.5\,]^T \text{ deg/s}$$

The aforementioned tracking maneuver is simulated using the proposed backstepping control law with the gains being $s = 0.001$, $g = 2.0$, $\alpha = 0.75$, $\beta = 8.0$, and $\eta = 1.0$. With the given choice of the control gains, we get the analytical upper bound norm $\|\boldsymbol{T}_{\text{analytical}}\|$ as 28.3019 N · m and the settling time t_{settling} as 24.7576 s, where t_{settling} is defined to be as the time at and after which the norm of the error states vector $[\,\boldsymbol{\sigma}_v^T, \quad \delta\boldsymbol{\omega}^T\,]^T$ is bounded by 1% error from the steady state of zero. Because the peak Euclidean norm of the actual control torque from the simulation, $\max(\|\boldsymbol{T}\|_2)$, is about 3.9820 N · m, the bound given by Eq. (26) is 7.1075 times bigger than the actual maximum torque. As for the stabilization example, the same optimization problem is solved subject to $t_{\text{settling}} \leq 13$ s and the closed-loop dynamics. The values of the gains s, g, α, β, and η given above are chosen as the starting guess and, as a result of optimization, these values converged to 0.1673, 12.1032, 0.2277, 20.9253, and 4, respectively. Figures 2a–2d show the simulation results for these converged values of the gains employed in the controller given by Eq. (19). The resulting analytical upper bound norm $\|\boldsymbol{T}_{\text{analytical}}\|$ is about 7.2799 N · m. The conservativeness of the upper bound is reduced from 7.1075 to 4.029 times bigger than the actual maximum Euclidean norm of control torque of 1.8069 N · m while significantly improving the settling time from 24.7576 to 13 s. Again, the optimized bound guarantees that the actual control torque never exceeds the bound with the condition that $|e_i(t_0)|$ is less than or equal to the value for the current scenario.

Conclusions

We addressed the issue of reducing the peak control torque for the attitude maneuver problem of a spacecraft by introducing a new positive constant gain within the framework of conventional integrator backstepping-based control design. The bounds for the control torque components are derived analytically as a function of the initial tracking error and the gains involved in the control design procedure. The proposed controller has been shown to perform adequately in the numerical simulations. We also demonstrated that the analytical bound can be used for reducing the guaranteed maximum torque upper bound.

References

[1] Khalil, H. K., *Nonlinear Systems*, 3rd ed., Prentice—Hall, Upper Saddle River, NJ, 2002, Chap. 14.

[2] Kanellakopoulos, I., Kokotovic, P. V., and Morse, A. S., "A Toolkit for Nonlinear Feedback Design," *Systems and Control Letters*, Vol. 18, 1992, pp. 83–92. doi:10.1016/0167-6911(92)90012-H

[3] Krstić, M., and Tsiotras, P., "Inverse Optimal Stabilization of a Rigid Spacecraft," *IEEE Transactions on Automatic Control*, Vol. 44, No. 5, 1999, pp. 1042–1049. doi:10.1109/9.763225

[4] Kim, K.-S., and Kim, Y., "Robust Backstepping Control for Slew Maneuver Using Nonlinear Tracking Function," *IEEE Transactions on Control Systems Technology*, Vol. 11, No. 6, 2003, pp. 822–829. doi:10.1109/TCST.2003.815608

[5] Sontag, E. D., and Sussmann, H. J., "Further Comments on the Stabilizability of the Angular Velocity of a Rigid Body," *Systems and Control Letters*, Vol. 12, 1989, pp. 213–217. doi:10.1016/0167-6911(89)90052-2

[6] Wie, B., and Lu, J., "Feedback Control Logic for Spacecraft Eigenaxis Rotations Under Slew Rate and Control Constraints," *Journal of Guidance, Control, and Dynamics*, Vol. 18, No. 6, 1995, pp. 1372–1379. doi:10.2514/3.21555

[7] Robinett, R. D., Parker, G. G., Schaub, H., and Junkins, J. L., "Lyapunov Optimal Saturated Control for Nonlinear Systems," *Journal of Guidance, Control, and Dynamics*, Vol. 20, No. 6, 1997, pp. 1083–1088. doi:10.2514/2.4189

[8] Bošković, J. D., Li, S.-M., and Mehra, R. K., "Globally Stable Adaptive Tracking Control Design for Spacecraft Under Input Saturation," *Proceedings of the 1999 IEEE Conference on Decision and Control*, Vol. 2, IEEE Press, Piscataway, NJ, 1999, pp. 1952–1957. doi:10.1109/CDC.1999.830922

[9] Bošković, J. D., Li, S.-M., and Mehra, R. K., "Robust Adaptive Variable Structure Control of Spacecraft Under Control Input Saturation," *Journal of Guidance, Control, and Dynamics*, Vol. 24, No. 1, 2001, pp. 14–22. doi:10.2514/2.4704

[10] Bošković, J. D., Li, S.-M., and Mehra, R. K., "Robust Tracking Control Design for Spacecraft Under Control Input Saturation," *Journal of Guidance, Control, and Dynamics*, Vol. 27, No. 4, 2004, pp. 627–633. doi:10.2514/1.1059

[11] Wallsgrove, R. J., and Akella, M. R., "Globally Stabilizing Saturated Attitude Control in the Presence of Bounded Unknown Disturbances," *Journal of Guidance, Control, and Dynamics*, Vol. 28, No. 5, 2005, pp. 957–963. doi:10.2514/1.9980

[12] Mazenc, F., and Iggidr, A., "Backstepping with Bounded Feedbacks," *Systems and Control Letters*, Vol. 51, 2004, pp. 235–245. doi:10.1016/j.sysconle.2003.09.001

[13] Shuster, M. D., "A Survey of Attitude Representations," *Journal of the Astronautical Sciences*, Vol. 41, No. 4, 1993, pp. 439–517.

[14] Schaub, H., and Junkins, J. L., *Analytical Mechanics of Space Systems*, AIAA Education Series, AIAA, Reston, VA, 2003, pp. 314, 324–325.

[15] Luo, W., Chu, Y.-C., and Ling, K.-V., "Inverse Optimal Adaptive Control for Attitude Tracking of Spacecraft," *IEEE Transactions on Automatic Control*, Vol. 50, No. 11, Nov. 2005, pp. 1639–1654. doi:10.1109/TAC.2005.858694

[16] Tsiotras, P., "Further Passivity Results for the Attitude Control Problem," *IEEE Transactions on Automatic Control*, Vol. 43, No. 11, Nov. 1998, pp. 1597–1600. doi:10.1109/9.728877

[17] Seo, D., and Akella, M. R., "Separation Property for the Rigid-Body Attitude Tracking Control Problem," *Journal of Guidance, Control, and Dynamics*, Vol. 30, No. 6, 2007, pp. 1569–1576. doi:10.2514/1.30296

[18] Wen, J. T., and Kreutz-Delgado, K., "Attitude Control Problem," *IEEE Transactions on Automatic Control*, Vol. 36, No. 10, 1991, pp. 1148–1162. doi:10.1109/9.90228

[19] Bhat, S. P., and Bernstein, D. S., "Topological Obstruction to Continuous Global Stabilization of Rotational Motion and the Unwinding Phenomenon," *Systems and Control Letters*, Vol. 39, No. 1, Jan. 2000, pp. 63–70. doi:10.1016/S0167-6911(99)00090-0

[20] Wie, B., and Barba, P. M., "Quaternion Feedback for Spacecraft Large Angle Maneuvers," *Journal of Guidance, Control, and Dynamics*,

Vol. 8, No. 3, 1985, pp. 360–365.
doi:10.2514/3.19988

[21] Joshi, S. M., Kelkar, A. G., and Wen, J. T.-Y., "Robust Attitude Stabilization of Spacecraft Using Nonlinear Quaternion Feedback," *IEEE Transactions on Automatic Control*, Vol. 40, No. 10, 1995, pp. 1800–1803.
doi:10.1109/9.467669

[22] Schaub, H., Robinett, R. D., and Junkins, J. L., "Globally Stable Feedback Laws for Near-Minimum-Fuel and Near-Minimum-Time Pointing Maneuvers for a Landmark-Tracking Spacecraft," *Journal of the Astronautical Sciences*, Vol. 44, No. 4, 1996, pp. 443–466.